Molecular Dynamics Investigation of Polytetrafluoroethylene Coating on Al2O3/Cr2O3/Ti2O3 for Cavitation Erosion Mitigation in Water Hydraulics Valves

Masoud Kamoleka Mlela, He Xu, Haihang Wang and Vishwanath Pooneeth

Molecular Dynamics Investigation of Polytetrafluoroethylene Coating on Al_2O_3/Cr_2O_3/Ti_2O_3 for Cavitation Erosion Mitigation in Water Hydraulics Valves

Masoud Kamoleka Mlela [1, a], He Xu[2,b], Haihang Wang[3,c] and Vishwanath Pooneeth[4,d]

Harbin Engineering University, College of Mechanical and Electrical Engineering, Harbin, China.

[a]masoudkamoleka@gmail.com, [b]railway_dragon@163.com, [c]wanghaihang@hrbeu.edu.cn, [d]vpooneeth@ymail.com

Abstract. Impairment caused by cavitation erosion and abrasive wear in valves is a significant problem for water hydraulic machinery in both underwater and industrial application. Material chemistry plays a major role in eliminating this cavitation erosion phenomenon. A Coating study of polytetrafluoroethylene (PTFE) on (1 0 0), (0 1 0) and (0 0 1) surface of Al_2O_3, Cr_2O_3 and Ti_2O_3 using molecular dynamics (MD) simulation that was conducted by Materials Studio (MS) discover code under similar initial conditions. PTFE layer was set on the cleaved planes (1 0 0) and (0 1 0) was more likely absorbed firmly on the surface of Al_2O_3 powder than that of Cr_2O_3 and Ti_2O_3 simply because of the binding energy of PTFE/Al_2O_3 being larger than that of PTFE/Cr_2O_3 and PTFE/Ti_2O_3. It has been studied that the composite coating of the PTFE on the (0 1 0) surface of Al_2O_3 became harder compared with PTFE/Al_2O_3 cleaved along (1 0 0) plane and PTFE/Cr_2O_3 cleaved along (0 0 1) plane in the magnitude order of 3188.006 > 1882.626 >1364.538 kJ/mol. The PTFE interacts mainly through electrostatic force in all (1 0 0), (0 1 0) and (0 0 1) surface of Al_2O_3. Meanwhile, it was observed that the PTFE adsorbed mainly with the use of electrostatic force on (1 0 0), (0 0 1) surface of Cr_2O_3, and (0 1 0) surface of Cr_2O_3 dominated by Van der Waals'force. In this work, concluded that the greater the binding energy the higher the hardness that mighty absorbs bubbles' imploding energies, hence mitigating the valve cavitation damage at a certain threshold value.

I. Introduction

Improving the excellence of materials, as well as their operational uniqueness becomes predominantly important now. It is very important to develop engineering materials with high erosion resistance to minimize cavitation erosion [1]. The hydraulic system that uses water as an alternative of oil as a pressure transmitting medium has been of great interest to researchers in recent years is environmentally friendly, non-combustible, low-cost, sanitary, readily available, and easily reusable if compared to oil hydraulics[2]. The synergistic erosion damage caused by cavitation, abrasive wear, and corrosion is a common and serious problem for hydraulic and marine machinery in rivers and oceans with high concentrations of sediment, especially valves, turbines, pumps, and propellers [3]. From the perspective of material properties, the issue of high strength and toughness, as well as high corrosion resistance in seawater, has recently grown in importance to enhance cavitation erosion resistance. In that case, numerous varieties of ceramic coatings have been applied to improve cavitation erosion resistance through various coating processes [4]. It is well acknowledged that abrasive wear rate of a surface is inversely proportional to its hardness [5]. Moreover, hardness measured as the material ability to refuse to accept to elastic and plastic deformations or to a brittle fracture [6]. The use of conducting polymer coatings has found success in the corrosion protection of metal [7]. According to density function theory, the chemical potential μ, the electronegativity of χ, the hardness η and the softness S of the chemical species is given by equation (1), depicted by Gazquez *at. al* in [8, 9]

$$\mu = -\chi = \left(\frac{\partial E}{\partial N}\right)_{v(r)} \tag{1.}$$

Allison and Tong in [10]described Fukui function and related chemical reactivity functions within the framework of density functional theory (DFT). Potential energy changes as the reactant approach molecules, this may be caused by the transfer of electrons to and from a reactant or due to its change in the geometric structure of the molecule. This can be analysed using the concepts from DFT, energy change may be termed as in equation (2)

$$dE = \left(\frac{\partial E}{\partial N}\right)_{v(r)} dN + \int \left(\frac{\partial E}{\partial V(r)}\right)_N \partial v(r) dr \tag{2.}$$

where E is the energy, N is the number of electrons, and $v(\mathbf{r})$ is the external potential at some point $\mathbf{r}$. The second term is equal to the electron density, $\rho(r)$ as equation (3) portray the change in the energy due to the change of the external potential at a fixed number of electrons.

$$\rho(r) = \left(\frac{\partial E}{\partial V(r)}\right)_N \tag{3.}$$

Correlation of energy and hardness arises as the terms of interest which describe the hardness (η) equal to the second derivative of energy with respect to the number of electrons at constant external potential as equation (4) shows.

$$\eta = \left(\frac{\partial^2 E}{\partial N^2}\right)_{v(r)} \tag{4.}$$

II.   Simulation and Computation Details

Classical molecular dynamics simulation is appropriate for studying the structure and property relationships for large and complicated systems, and it is able to provide statistical and average results approximately[11]. The simulation computation was established using the material science simulation software named Material Studio® Software developed by Accelrys Software Inc. after doing several steps of model construction and calculation. The tasks were to build optimized of slabs of Al_2O_3, Cr_2O_3 and Ti_2O_3 each in a cleaved plane along (1 0 0), (0 1 0) and (0 0 1) with an identical thickness of 13.233 $\overset{\circ}{A}$ each. By smarter Algorithm with a maximum iteration of 100,000 steps, the surfaces were relaxed at minimal energy with the aid typing of the model based on *ab initio* data the condensed-phase optimized molecular potentials for atomistic simulation studies (COMPASS) forcefield was used to assure bond between the metal oxide (Al_2O_3, Cr_2O_3, and Ti_2O_3) exist. The supercell was built by increasing the surface to U×V=6×6 and followed by to build the slab without the vacuum aim to change the periodicity from 2D to 3D. The steps of making a slab are identical to all selected metal-oxides (Al_2O_3, Cr_2O_3, and Ti_2O_3). The periodic layer of the amorphous cell of polytetrafluoroethylene (PTFE) constructed and a geometry refinement of the structure was performed from an atactic polymer that was used in this work simulation. This is prebuilt imported from the repeat-unit tetrafluoroethylene of chain length of 50 with a number of configurations fixed to 1.0, the target density of final configurations agreed to 2g/cm³. Next step is to build a layer of coating of respective minimized polytetrafluoroethylene on optimized the selected metal-oxides surface in the subsequence job of MS, this was achieved by creating a vacuum of 70 for polytetrafluoroethylene that will match with the metal-oxide slabs. The aim was to obtain the
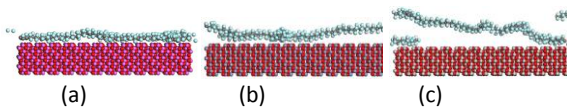

(a)   (b)   (c)

Fig. 1. The equilibrium structures on the 6×6 cleaved (1 0 0) face of (a) PTFE/Al₂O₃ (b) PTFE/Cr₂O₃ (c) PTFE/Ti₂O₃

(a)   (b)   (c)

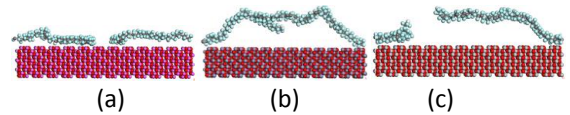**Fig. 2.** The equilibrium structures on the 6×6 cleaved (0 1 0) face of (a) PTFE/Al₂O₃ (b) PTFE/Cr₂O₃ (c) PTFE/Ti₂O₃

model structure of (6×6) layer of PTFE/Al$_2$O$_3$(1 0 0), PTFE/Cr$_2$O$_3$(1 0 0), PTFE/Ti$_2$O$_3$(1 0 0), PTFE/Al$_2$O$_3$(0 1 0), PTFE/Cr$_2$O$_3$(0 1 0), PTFE/Ti$_2$O$_3$(0 1 0), PTFE/Al$_2$O$_3$(0 0 1), PTFE/Cr$_2$O$_3$(0 0 1), PTFE/Ti$_2$O$_3$(0 0 1).the energy minimization, MD simulations were performed in each Composite layer (polytetrafluoroethylene _Al$_2$O$_3$((1 0 0), (0 1 0), (0 0 1))/Cr$_2$O$_3$((1 0 0), (0 1 0), (0 0 1))/Ti$_2$O$_3$((1 0 0), (0 1 0), (0 0 1)). The simulation carried out at room temperature (298K), Andersen temperature control method was selected, using the ensembles of a constant number of particles, constant volume and constant temperature (NVT). In each case, the simulation was performed with an interval of 1 femtosecond (fs) and the simulation steps were 200,000 with a total dynamic time of 200.0 picoseconds (ps). Meanwhile, in each case and dynamic atom configurations were saved as trajectories every 5000 frames. Consequently, the interaction energy and binding energy can be calculated by equation (5)

$$E_{binding} = -E_{interaction} = -[E_{total} - (E_{surface} + E_{polymer})] \qquad (5.)$$

Where $E_{interaction}$ is the interaction energy of the equilibrated structure, E_{total} is the single-point total energy of the equilibrated structure after the interaction, $E_{surface}$ is the single point energy of the oxide surface before interaction with the polymer, and $E_{polymer}$ is the single point energy of the polymer.

III. Results and Discussions

A model was to calculate and compare the interaction energies of the composite coating layer of the equilibrated structure of PTFE on the (1 0 0), (0 1 0), and (0 0 1) crystalline surface of Al$_2$O$_3$, Cr$_2$O$_3$ and Ti$_2$O$_3$ individually. In this work, MD method was used to investigate the material properties in terms of hardness through binding energy to withstand the cavitation effect of bubbles imploding in the walls of the inner structure of water hydraulics components such as valves, hydro-turbines and pumps. The three designed schemes of coating reaction are presented in Fig. 1, 2, and 3. When the interaction bond is strong, there is higher binding energy because it takes more energy to break a strong bond. Table 1, 2, and 3 show the results obtained from the Molecular Dynamic simulation of the equilibrated systems to examine the most stable and strong bond layer in terms of hardness correlated with the minimum energy from simulation results. The results, as seen from Table 1 extracted from MD simulation of the cleaved plane along (1 0 0) in the arrangements of Fig. 1 above indicate that the binding energy of PTFE on Al$_2$O$_3$, Cr$_2$O$_3$ and Ti$_2$O$_3$ (1 0 0) surfaces are 1882.626, 275.577 and 77.188 kcal/mol respectively. Consequently, the results show the strong evidence that the interaction of polymer and surface is dominated by electrostatic force in PTFE/Al$_2$O$_3$ and PTFE/Cr$_2$O$_3$ systems, but PTFE/Ti$_2$O$_3$ dominated by the vdW force. The binding energy determines the strength of the bond formed between the substrate and sorbate. PTFE/Al$_2$O$_3$>PTFE/Cr$_2$O$_3$>PTFE/Ti$_2$O$_3$ is the order of high to low energy in the layer PTFE/Al$_2$O$_3$ is larger than that of the analysed structure

Table 1: The interaction energy of PTFE on the surface of the 6×6 crystal structure of (1 0 0) metal-oxides (Al$_2$O$_3$, Cr$_2$O$_3$, and Ti$_2$O$_3$) at 298K

Composite (1 0 0)		E$_t$(kJ/mol)	E$_s$(kJ/mol)	E$_p$(kJ/mol)	E$_{int}$(kJ/mol)	E$_b$(kJ/mol)
PTFE on Al$_2$O$_3$	E	1503645.646	1504701.171	827.102	-1882.626	1882.626
	vdW	1819595.144	1819534.868	234.719	-174.443	174.443
	Electrostatic	-316394.743	-314833.697	147.137	-1708.183	1708.183
PTFE on Cr$_2$O$_3$	E	-2044424.273	-2043371.693	-777.003	-275.577	275.577
	vdW	-1718384.934	-1718389.935	66.943	-61.942	61.942
	Electrostatic	-325245.070	-324981.758	-49.676	-213.636	213.636
PTFE on Ti$_2$O$_3$	E	3.62E+14	3.62E+14	-799.816	-77.188	77.188
	vdW	3.62E+14	3.62E+14	62.966	-42.938	42.938
	Electrostatic	-270568.263	-270280.741	-253.766	-33.756	33.756

Annotation: E$_t$ is the single-point total energy of the equilibrated structure (1 0 0), E$_p$ is the single-point energy of the polytetrafluoroethylene, E$_s$ is a single-point energy of the surface (Al$_2$O$_3$, Cr$_2$O$_3$ and Ti$_2$O$_3$), E$_{int}$ is the interaction energy of the equilibrated structure, E$_b$ is the binding energy of the equilibrated structure, E is the total energy of each structure, vdW is the energy of each structure attained by vdW force, electrostatic is the energy of each structure attained by electrostatic force.

Table 2: The interaction energy of PTFE on the surface of the 6×6 crystal structure of (0 1 0) metal-oxides (Al_2O_3, Cr_2O_3, and Ti_2O_3) at 298K

Composite (0 1 0)		E_t (kJ/mol)	E_s (kJ/mol)	E_p (kJ/mol)	E_{int} (kJ/mol)	E_b (kJ/mol)
PTFE on Al_2O_3	E	1502468.414	1504701.171	955.249	-3188.006	3188.006
	vdW	1819660.120	1819534.868	239.698	-114.447	114.447
	Electrostatic	-317576.451	-314833.697	330.805	-3073.559	3073.559
PTFE on Cr_2O_3	E	-2043990.563	-2043371.693	-610.956	-7.914	7.914
	vdW	-1718330.744	-1718389.935	72.878	-13.688	13.688
	Electrostatic	-325037.155	-324981.758	-61.171	5.774	-5.774
PTFE on Ti_2O_3	E	3.62E+14	3.62E+14	-780.251	-1.750	1.750
	vdW	3.62E+14	3.62E+14	80.948	-8.938	8.938
	Electrostatic	-270345.255	-270280.741	-71.428	6.913	-6.913

Annotation: E_t is the single-point total energy of the equilibrated structure (0 1 0), E_p is the single-point energy of the polytetrafluoroethylene, E_s is a single-point energy of the surface (Al_2O_3, Cr_2O_3 and Ti_2O_3), E_{int} is the interaction energy of the equilibrated structure, E_b is the binding energy of the equilibrated structure, E is the total energy of each structure, vdW is the energy of each structure attained by vdW force, electrostatic is the energy of each structure attained by electrostatic force.

of PTFE/Cr_2O_3 and PTFE/Ti_2O_3. Data gathered from further MD simulation of the cleaved plane along (0 1 0) face as seen in Fig. 2 stipulated in Table 2. The binding energy of PTFE on Al_2O_3, Cr_2O_3 and Ti_2O_3 surfaces are 3188.006, 7.914 and 1.750 kcal/mol respectively. Again, the binding energy of the composite of PTFE/Al_2O_3 seems to be large than PTFE/Cr_2O_3 and PTFE/Ti_2O_3 and all the binding energy from the cleaved plane along (1 0 0), (0 1 0) and (0 0 1) faces. The MD simulation results from the arrangement in the Fig. 2 denote that, PTFE/Ti_2O_3 is the low binding energy surface compared to PTFE/Cr_2O_3 and PTFE/Al_2O_3 in the order of PTFE/Al_2O_3>PTFE/Cr_2O_3> PTFE/Ti_2O_3. Final MD simulation arrangements of the cleaved plane along (0 0 1) face as seen in Fig.3 provide the results in Table 3. The results show that the binding energy of PTFE on Al_2O_3, Cr_2O_3 and Ti_2O_3 surfaces are 655.419, 1364.538 and 712.784 kcal/mol respectively. The results show that the PTFE/Al_2O_3 is the low binding energy surface compared to PTFE/Cr_2O_3 and PTFE/Al_2O_3 in the order of PTFE/Cr_2O_3>PTFE/Ti_2O_3>PTFE/Al_2O_3. Moreover, the overall binding energy of the PTFE/Al_2O_3 cleaved along (0 1 0) plane observed to be larger than all the binding energy from the cleaved plane along (0 0 1) (1 0 0) and (0 0 1). Next followed by PTFE/Al_2O_3 cleaved along (1 0 0) plane and PTFE/Cr_2O_3 cleaved along (0 0 1) plane in the magnitude order of 3188.006 > 1882.626 > 1364.538 kJ/mol. It is well known that the energy or work done required to pull nuclear apart into its constituent or disassemble the nucleus is equal to the binding energy. Since the bubbles cloud collapsing and explode at about the maximum hydrostatic pressure of 1000MPa[12] at the walls of water hydraulic components, consider the case of valves. in turn, the relationship between pressure and energy is signified in the equation (6) below.
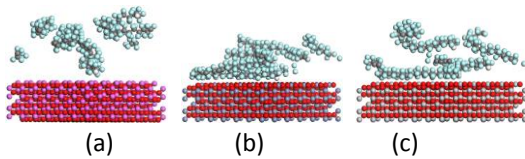

Fig. 3. The equilibrium structures on the 6×6 cleaved (0 0 1) face of (a) PTFE/Al_2O_3 (b) PTFE/Cr_2O_3 (c) PTFE/Ti_2O_3

$$Pressure(Pa) = \frac{F(N)}{A(m^2)} = \frac{F(N) \times d(m)}{A(m^2) \times d(m)} = \frac{Work\ done(J)}{Volume(m^3)} \quad (6.)$$

$$P(Pa) \times V(m^3) < Binding\ Energy \quad (7.)$$

Where F is a force, and A is a cross-section area. In order, the water hydraulic machinery components to be protected from the cavitation effect, the following condition must be fulfilled where P is the pressure and V is the volume of the water hydraulic valves for water passage. Correspondingly, volume (V) determine the size of the water hydraulic system. From the correlation shown in the equation (7), it is clearly studied that the cavitation effect suppression depends mainly on the strength of the bond or binding energy between composite layers, the large the binding energy the less the possibility of cavitation wear and erosion. The correlation also depicts the wear can be accelerated by excessive pressure fluctuations beyond the certain

Table 3: The interaction energy of PTFE on the surface of the 6×6 crystal structure of (0 0 1) Metal-Oxides (Al_2O_3, Cr_2O_3, And Ti_2O_3) at 298K

Composite (0 0 1)		E_t (kJ/mol)	E_s (kJ/mol)	E_p(kJ/mol)	E_{int}(kJ/mol)	E_b(kJ/mol)
PTFE on Al_2O_3	E	-729015.068	-727482.268	-877.380	-655.419	655.419
	vdW	-615116.852	-615184.729	74.028	-6.152	6.152
	Electrostatic	-113137.003	-112297.540	-190.195	-649.268	649.268
PTFE on Cr_2O_3	E	-505085.055	-504256.648	536.131	-1364.538	1364.538
	vdW	-496826.095	-496912.047	161.762	-75.810	75.810
	Electrostatic	-8364.824	-7344.601	268.505	-1288.728	1288.728
PTFE on Ti_2O_3	E	-540025.741	-539492.522	179.565	-712.784	712.784
	vdW	-510864.795	-511019.007	170.419	-16.207	16.207
	Electrostatic	-29085.998	-28473.515	84.094	-696.577	696.577

Annotation: E_t is the single-point total energy of the equilibrated structure (0 0 1), E_p is the single-point energy of the polytetrafluoroethylene, E_s is a single-point energy of the surface (Al_2O_3, Cr_2O_3 and Ti_2O_3), E_{int} is the interaction energy of the equilibrated structure, E_b is the binding energy of the equilibrated structure, E is the total energy of each structure, vdW is the energy of each structure attained by vdW force, electrostatic is the energy of each structure attained by electrostatic force.

value in the valve, pump chamber and other water hydraulic components that are vulnerable to cavitation erosion due to exploding of cavitation bubbles.

Another factor might be, the larger the volume flow rate is more susceptible to cavitation erosion phenomenon. The equation (7) agreed with the postulates introduced by R. Singh *at al*., [12], he argued that the cavitation erosion is measured or predicted from the impact energy of the bubble collapse.

$$\sigma = (P - P_v) \big/ (\tfrac{1}{2} \rho v^2) \quad = (P - P_v) \big/ (\tfrac{1}{2} \frac{m}{V} v^2) \tag{8.}$$

Further, through equation (8) he declared that cavitation impacts with the energy larger than a certain threshold level would cause the erosion of the materials. That means the threshold impacts of the of the bubble collapse are significant as they initiate fatigue fracture of the surface.

IV. Conclusions

In this study, It has been conclusively shown that the structure of $PTFE/Al_2O_3$ of face (0 1 0) composite can highly withstand wear effect caused by the imploding of water cavitation bubbles a certain large threshold value in the water hydraulics valves compared to another system of polymer/metal-oxides composite analysed in this study. The increase in cavitation erosion resistance can mainly attributed to the increase in hardness and to the elastic response of the expanded of $PTFE/Al_2O_3$. Consequently, equation (4) gives the correlation between energy and hardness. It is definitely that, PTFE is more likely absorbed firmly on the surface of the Al_2O_3 powder than that of Cr_2O_3 and Ti_2O_3 simply because of the binding energy of $PTFE/Al_2O_3$ in all three cleaved planes (1 0 0), (0 1 0) and (0 0 1) is larger than that of $PTFE/Cr_2O_3$ and $PTFE/Ti_2O_3$. It was declared that PTFE has larger coating strength on Al_2O_3 compared to that of Ti_2O_3 and Cr_2O_3. It is clearly results in the tables' show that the contribution of electrostatic forces to the larger binding energies obtained are larger than the contribution of the van der Waals force.

V. Acknowledgement

VI. References

[1] T. Zhang, C. Chen, D. Lu, and D. Li, "Mechanism of silt abrasion enhanced by cavitation in silt laden water flow," *Paiguan Jixie Gongcheng Xuebao/Journal of Drainage and Irrigation Machinery Engineering,* vol. 29, no. 4, pp. 297-302, 2011.

[2] S. Weijie, C. Shuping, L. Xiaohui, Z. Zuti, and Z. Yuquan, "Experimental Research on the Cavitation Suppression in the Water Hydraulic Throttle Valve," *Journal of Pressure Vessel Technology, Transactions of the ASME,* vol. 139, no. 5, 2017.

[3] W. Gou, H. Zhang, H. Li, F. Liu, and J. Lian, "Effects of silica sand on synergistic erosion caused by cavitation, abrasion, and corrosion," *Wear,* vol. 412-413, pp. 120-126, 2018/10/15/ 2018.

[4] Y. J. Kim, J. W. Jang, D. W. Lee, and S. Yi, "Porosity effects of a Fe-based amorphous/nanocrystals coating prepared by a commercial high velocity oxy-fuel process on cavitation erosion behaviors," *Metals and Materials International,* vol. 21, no. 4, pp. 673-677, 2015/07/01 2015.

[5] C. S. Ramesh, C. K. Srinivas, and B. H. Channabasappa, "Abrasive wear behaviour of laser sintered iron–SiC composites," *Wear,* vol. 267, no. 11, pp. 1777-1783, 2009/10/29/ 2009.

[6] V. A. Mukhanov, O. O. Kurakevych, and V. L. Solozhenko, "The interrelation between hardness and compressibility of substances and their structure and thermodynamic properties," *Journal of Superhard Materials,* journal article vol. 30, no. 6, p. 368, January 09 2009.

[7] A. Kausar, "Polymer coating technology for high performance applications: Fundamentals and advances," *Journal of Macromolecular Science, Part A,* vol. 55, no. 5, pp. 440-448, 2018/05/04 2018.

[8] J. L. Gazquez, A. Martinez, and F. Mendez, "Relationship between energy and hardness differences," *The Journal of Physical Chemistry,* vol. 97, no. 16, pp. 4059-4063, 1993/04/01 1993.

[9] J. L. Gázquez, "Bond Energies and Hardness Differences," *The Journal of Physical Chemistry A,* vol. 101, no. 49, pp. 9464-9469, 1997/12/01 1997.

[10] T. C. Allison and Y. J. Tong, "Application of the condensed Fukui function to predict reactivity in core–shell transition metal nanoparticles," *Electrochimica Acta,* vol. 101, pp. 334-340, 2013/07/01/ 2013.

[11] J. Xiao *et al.*, *Molecular dynamics study on the relationships of modeling, structural and energy properties with sensitivity for RDX-based PBXs*. 2012.

[12] R. Singh, S. K. Tiwari, and S. K. Mishra, "Cavitation Erosion in Hydraulic Turbine Components and Mitigation by Coatings: Current Status and Future Needs," *Journal of Materials Engineering and Performance,* vol. 21, no. 7, pp. 1539-1551, 2012/07/01 2012.